

DRAFT: First Measurement of the Double Spin Asymmetry in
 $\vec{e}\vec{p} \rightarrow e'\pi^+n$ in the Resonance Region

R. DeVita,¹ M. Anghinolfi,¹ M. Battaglieri,¹ V.D. Burkert,² G.E. Dodge,³ R. Minehart,⁴
M. Ripani,¹ M. Taiuti,¹ H. Weller,⁵ G. Adams,³⁰ M.J. Amarian,³⁷ E. Anciant,¹¹
D.S. Armstrong,³⁶ B. Asavapibhop,²⁴ G. Asryan,³⁷ G. Audit,¹¹ T. Auger,¹¹ H. Avakian,¹⁸
S. Barrow,¹⁶ K. Beard,²¹ M. Bektasoglu,³ B.L. Berman,¹⁷ W. Bertozzi,²³ N. Bianchi,¹⁸
A.S. Biselli,³⁰ S. Boiarinov,²⁰ B.E. Bonner,³¹ P. Bosted,⁶ S. Bouchigny,² D. Branford,¹⁴
W.J. Briscoe,¹⁷ W.K. Brooks,² S. Bueltmann,⁴ J.R. Calarco,²⁶ G.P. Capitani,¹⁸
D.S. Carman,⁹ B. Carnahan,¹⁰ C. Cetina,¹⁷ L. Ciciani,³ R. Clark,⁹ P.L. Cole,^{34, 2}
A. Coleman,³⁶ J. Connelly,¹⁷ D. Cords,² P. Corvisiero,¹ D. Crabb,⁴ H. Crannell,¹⁰
J.P. Cummings,³⁰ E. DeSanctis,¹⁸ P.V. Degtyarenko,^{2, 20} R. Demirchyan,³⁷ L. Dennis,¹⁶
K.S. Dhuga,¹⁷ C. Djalali,³³ J. Domingo,² D. Doughty,^{12, 2} P. Dragovitsch,¹⁶ M. Dugger,⁷
S. Dytman,²⁹ M. Eckhause,³⁶ Y. Efremenko,²⁰ H. Egiyan,³⁶ K.S. Egiyan,³⁷
L. Elouadrhiri,^{12, 2} A. Empl,³⁰ L. Farhi,¹¹ R. Fatemi,⁴ R.J. Feuerbach,⁹ J. Ficenec,³⁵
T.A. Forest,³ V. Frolov,³⁰ H. Funsten,³⁶ S.J. Gaff,⁵ M. Gai,¹³ G. Gavalian,³⁷ V. Gavrilov,²⁰
S. Gilad,²³ G.P. Gilfoyle,³² K.L. Giovanetti,²¹ P. Girard,³³ E. Golovatch,²⁵ K. Griffioen,³⁶
M. Guidal,^{19, 11} M. Guillo,³³ V. Gyurjyan,² D. Hancock,³⁶ J. Hardie,¹² D. Heddle,^{12, 2}
P. Heimberg,¹⁷ J. Heisenberg,²⁶ F.W. Hersman,²⁶ K. Hicks,²⁸ R.S. Hicks,²⁴ M. Holtrop,²⁶
J. Hu,³⁰ C.E. Hyde-Wright,³ M.M. Ito,² D. Jenkins,³⁵ K. Joo,⁴ J.H. Kelley,⁵
M. Khandaker,²⁷ D.H. Kim,²² K.Y. Kim,²⁹ K. Kim,²² W. Kim,²² A. Klein,³ F.J. Klein,¹⁰
M. Klusman,³⁰ M. Kossov,²⁰ L.H. Kramer,^{15, 2} Y. Kuang,³⁶ S.E. Kuhn,³ J.M. Laget,¹¹
D. Lawrence,²⁴ G.A. Laksin,²⁰ A. Longhi,¹⁰ K. Loukachine,^{2, 35} M. Lucas,³³ W. Major,³²
J.J. Manak,² C. Marchand,¹¹ S.K. Matthews,¹⁰ L.C. Maximon,¹⁷ S. McAleer,¹⁶
J. McCarthy,⁴ J.W.C. McNabb,⁹ B.A. Mecking,² M.D. Mestayer,² C.A. Meyer,⁹
M. Mirazita,¹⁸ R. Miskimen,²⁴ V. Mokeev,²⁵ V. Muccifora,¹⁸ J. Mueller,²⁹ L.Y. Murphy,¹⁷
G.S. Mutchler,³¹ J. Napolitano,³⁰ S.O. Nelson,⁵ G. Niculescu,²⁸ I. Niculescu,¹⁷

B.B. Niczyporuk,² R.A. Niyazov,³ J.T. O'Brien,¹⁰ G.V. O'Rielly,¹⁷ M. Ossipenko,²⁵
A.K. Opper,²⁸ K. Park,²² G. Peterson,²⁴ S.A. Philips,¹⁷ N. Pivnyuk,²⁰ D. Pocanic,⁴
O. Pogorelko,²⁰ E. Polli,¹⁸ B.M. Preedom,³³ J.W. Price,^{8, 30} L.M. Qin,³ B.A. Raue,^{15, 2}
G. Riccardi,¹⁶ G. Ricco,¹ B.G. Ritchie,⁷ S. Rock,⁶ F. Ronchetti,¹⁸ P. Rossi,¹⁸
D. Rowntree,²³ P.D. Rubin,³² K. Sabourov,⁵ C. Salgado,²⁷ V. Sapunenko,¹ M. Sargsyan,¹⁵
² R.A. Schumacher,⁹ V.S. Serov,²⁰ A. Shafi,¹⁷ Y.G. Sharabian,³⁷ J. Shaw,²⁴ S. Shuvalov,²⁰
S. Simionatto,¹⁷ A.V. Skabelin,²³ E.S. Smith,² T. Smith,²⁶ L.C. Smith,⁴ D.I. Sober,¹⁰
L. Sorrell,⁶ M. Spraker,⁵ S. Stepanyan,³⁷ P. Stoler,³⁰ I.I. Strakovsky,¹⁷ S. Taylor,³¹
D.J. Tedeschi,³³ R. Thompson,²⁹ M.F. Vineyard,³² A.V. Vlassov,²⁰ K. Wang,⁴
L.B. Weinstein,³ A. Weisberg,²⁸ D.P. Weygand,² C.S. Whisnant,³³ E. Wolin,² L. Yanik,¹⁷
A. Yegneswaran,² J. Yun,³ B. Zhang,²³ J. Zhao,²³ Z. Zhou,²³

(The CLAS Collaboration)

¹ *Istituto Nazionale di Fisica Nucleare, Sezione di Genova, e Dipartimento di Fisica
dell'Università, 16146 Genova, Italy*

² *Thomas Jefferson National Accelerator Laboratory, Newport News, Virginia 23606, USA*

³ *Old Dominion University, Department of Physics, Norfolk, Virginia 23529, USA*

⁴ *University of Virginia, Department of Physics, Charlottesville, Virginia 22901, USA*

⁵ *Duke University, Durham, North Carolina 27708-0305, USA*

⁶ *American University, Washington, D.C. 20016, USA*

⁷ *Arizona State University, Department of Physics and Astronomy, Tempe, Arizona 85287-1504,
USA*

⁸ *University of California at Los Angeles, Department of Physics, Los Angeles, California
90095-1547, USA*

⁹ *Carnegie Mellon University, Department of Physics, Pittsburgh, Pennsylvania 15213, USA*

¹⁰ *Catholic University of America, Department of Physics, Washington, D.C. 20064, USA*

¹¹ *CEA-Saclay, Service de Physique Nucléaire, F91191 Gif-sur-Yvette, Cedex, France*

¹² *Christopher Newport University, Newport News, Virginia 23606, USA*

¹³ *University of Connecticut, Department of Physics, Storrs, Connecticut 06269, USA*

- ¹⁴ *Edinburgh University, Department of Physics, Edinburgh EH9 3JZ, United Kingdom*
- ¹⁵ *Florida International University, Miami, Florida 33199, USA*
- ¹⁶ *Florida State University, Department of Physics, Tallahassee, Florida 32306, USA*
- ¹⁷ *The George Washington University, Department of Physics, Washington, DC 20052*
- ¹⁸ *Istituto Nazionale di Fisica Nucleare, Laboratori Nazionali di Frascati, P.O. 13, 00044
Frascati, Italy*
- ¹⁹ *Institut de Physique Nucleaire ORSAY, Orsay, France*
- ²⁰ *Institute of Theoretical and Experimental Physics, Moscow, 117259, Russia*
- ²¹ *James Madison University, Department of Physics, Harrisonburg, Virginia 22807, USA*
- ²² *Kungpook National University, Department of Physics, Taegu 702-701, South Korea*
- ²³ *Massachusetts Institute of Technology, Cambridge, Massachusetts 02139-4307, USA*
- ²⁴ *University of Massachusetts, Department of Physics, Amherst, Massachusetts 01003, USA*
- ²⁵ *University of Moscow, Moscow, 119899 Russia*
- ²⁶ *University of New Hampshire, Department of Physics, Durham, New Hampshirs 03824-3568,
USA*
- ²⁷ *Norfolk State University, Norfolk, Virginia 23504, USA*
- ²⁸ *Ohio University, Department of Physics, Athens, Ohio 45701, USA*
- ²⁹ *University of Pittsburgh, Pittsburgh, Pennsylvania 15260, USA*
- ³⁰ *Rensselaer Polytechnic Institute, Troy, New York 12180-3590, USA*
- ³¹ *Rice University, Houston, Texas 77005-1892, USA*
- ³² *University of Richmond, Richmond, Virginia 23173, USA*
- ³³ *University of South Carolina, Columbia, South Carolina 29208, USA*
- ³⁴ *University of Texas at El Paso, El Paso, Texas 79968, USA*
- ³⁵ *Virginia Polytechnic Institute and State University, Blacksburg, Virginia 24061-0435,
USA*
- ³⁶ *College of William and Mary, Williamsburg, Virginia 23187-8795, USA*
- ³⁷ *Yerevan Physics Institute, 375036 Yerevan, Armenia*

(September 18, 2001)

Abstract

The first measurement of the double spin asymmetry for exclusive single π^+ electroproduction from protons has been performed in Hall B at the Thomas Jefferson National Accelerator Facility using CLAS. A 2.6 GeV polarized electron beam was incident on a polarized solid NH_3 target. The double spin asymmetry A_{ep} was measured in the resonance region for a range of momentum transfer squared, $0.35 < Q^2 < 1.5 \text{ GeV}^2$, and for a range of the π^+ center-of-mass polar angle, $0.25 < \cos\theta^* < 1$. Comparison with predictions of phenomenological models shows strong sensitivity to resonance contributions. Helicity-1/2 transitions are found to be dominant in the second and third resonance regions. The measured asymmetry is consistent with a faster rise with Q^2 of the helicity asymmetry A_1 for the $F_{15}(1680)$ resonance than expected from the analysis of the unpolarized data.

PACS : 13.60.le, 13.88.+e, 14.40aq

Measurements of the spin structure of exclusive pion production reactions provide a new approach to an understanding of the structure of baryon resonances, which has been the subject of experimental and theoretical studies for many years. The nucleon and its resonant states can, in principle, be described by QCD in terms of their elementary constituents, i.e. quarks and gluons, but in practice phenomenological models continue to play a fundamental role in attempts to understand these systems. In electroproduction, the transition to resonant states is characterized by the transverse helicity amplitudes $A_{1/2}$ and $A_{3/2}$, and by the longitudinal amplitude $S_{1/2}$, where 1/2 and 3/2 refer to the total helicity of the γ^*N system. The Q^2 dependence of these amplitudes yields information on the spin structure of the transition and on the wave function of the excited state. Models of baryon resonances as the ones in Ref. [1–4] make predictions for these quantities and can be tested via comparison with the measured amplitudes. Single pion production has been one of the main sources of information for these studies. However, most of these experiments have been limited to the measurement of the unpolarized cross section and only recently have technological developments in polarized sources and targets opened new possibilities for the study of polarization observables, which can provide important new constraints for the extraction of the resonance parameters. Double polarization experiments directly measure the helicity structure of the reaction, allowing the separation of the helicity amplitudes $A_{1/2}$ and $A_{3/2}$ without the complex analysis of the full angular distribution that is necessary for unpolarized measurements.

Double spin observables in single pion photoproduction have been measured in recent photoproduction experiments at MAINZ [5], while only recoil polarization measurements have been performed in electroproduction [6]. In addition to a highly-polarized beam and target or recoil polarimeters, these measurements require a large acceptance detector to measure the full angular distribution of the outgoing pion and to compensate for the relatively low luminosity that polarized solid targets can tolerate.

The CEBAF Large Acceptance Spectrometer (CLAS) in Hall B at TJNAF provides the large angular coverage that is necessary for the study of resonance decays. It is a magnetic

spectrometer based on a six-coil torus magnet whose field is primarily oriented along the azimuthal direction. The particle detection system includes drift chambers for track reconstruction [7], scintillation counters for the time of flight measurement [9], Cerenkov counters for electron-pion discrimination [8], and electromagnetic calorimeters to identify electrons and neutrals [10]. Charged particles can be detected and identified for momenta down to 0.2 GeV. With the polarized target inserted in the field free region at the center of the detector, the acceptance for polar angles is restricted to two regions, $\theta < 50^\circ$ and $75^\circ < \theta < 105^\circ$.

Data were taken at a beam energy of 2.6 GeV. The electron beam with an average polarization of 70% was incident on a cylindrical 1.5 cm diameter 1 cm length target cell filled with solid NH_3 pellets. The beam helicity was flipped at a rate of 1 Hz in a pseudo-random sequence to minimize systematic effects. The target material was maintained at a temperature of 1 K in a 5 T magnetic field generated by a superconducting Helmholtz magnet with its axis on the beamline. A proton polarization of 50-70% parallel to the electron beam was obtained by Dynamic Nuclear Polarization. The scattered electron was detected by a coincidence of Cerenkov counter and electromagnetic calorimeter. The positive pion was identified in coincidence with the electron by comparing its momentum determined from the reconstructed track and its time of flight as measured by the TOF scintillators. A cut on the reconstructed missing mass from the $e'\pi^+$ system of $0.85 < M_x < 1.05$ GeV was used to select the exclusive $e\pi^+n$ final state (see Figure 1).

The cross section can be written as

$$\sigma = \sigma_0 + P_e\sigma_e + P_p\sigma_p + P_eP_p\sigma_{ep}, \quad (1)$$

where σ_0 is the unpolarized cross section and P_e and P_p refer to the electron and proton polarization, respectively. Data with different combinations of the electron and proton polarization were used to isolate the double spin term, σ_{ep} , and to extract the double spin asymmetry, defined as $A_{ep} = -\sigma_{ep}/\sigma_0$. After integrating over the azimuthal angle ϕ^* of the pion in the center-of-mass frame, this quantity can be parametrized as

$$A_{ep} = \sqrt{1 - \epsilon^2} \cos\theta_\gamma \frac{A_1 + \eta A_2}{1 + \epsilon R} \quad (2)$$

where ϵ is the virtual photon polarization, θ_γ is the angle between the target spin and the virtual-photon momentum direction, $\eta = \tan \theta_\gamma \sqrt{2\epsilon/(1+\epsilon)}$, and R is the longitudinal-transverse cross section ratio σ_L/σ_T . The structure function A_1 is the virtual photon helicity asymmetry,

$$A_1 = \frac{|A_{1/2}|^2 - |A_{3/2}|^2}{|A_{1/2}|^2 + |A_{3/2}|^2}, \quad (3)$$

while A_2 is a longitudinal-transverse interference term.

The $e'\pi^+n$ events were accumulated in bins of Q^2 , W , and $\cos\theta^*$. To increase statistics, the data were integrated over the azimuthal angle ϕ^* . Geometrical cuts were used to select the high efficiency regions of the detector excluding the edges of the Cerenkov counter and of the drift chambers, dead drift-chamber wires, and mal-functioning TOF scintillators. For each kinematics, the acceptance was analytically calculated by projecting these fiducial regions into the center-of-mass frame and was applied on an event-by-event basis. The systematic uncertainty on the asymmetry due to the acceptance evaluation was estimated to be $\sim 0.01 - 0.02$. The double spin asymmetry was then obtained as

$$A_{ep} = \frac{1}{fP_eP_p} \frac{N(\uparrow\downarrow) + N(\downarrow\uparrow) - N(\uparrow\uparrow) - N(\downarrow\downarrow)}{N(\uparrow\downarrow) + N(\downarrow\uparrow) + N(\uparrow\uparrow) + N(\downarrow\downarrow)}, \quad (4)$$

where the arrows in parenthesis refer to the electron and proton spin orientation, and f denotes the dilution factor for the NH_3 target. The asymmetry $(A_1 + \eta A_2)/(1 + \epsilon R)$ was extracted dividing the double spin asymmetry by the factor $\sqrt{1 - \epsilon^2} \cos \theta_\gamma$.

The dilution factor represents the fraction of events from polarized target nucleons and accounts for the contribution of the nuclear background from the liquid helium, ^{15}N , and vacuum windows in the target. Separate measurements on ^{12}C and liquid helium were used to model a nuclear background distribution shown as the dashed line in Figure 1. The background spectrum was normalized to the NH_3 spectrum in the tail of the missing mass peak ($M_x < 0.85$ GeV) where only nuclear reactions can contribute. The systematic error associated with this procedure was estimated to be ~ 0.04 . A subsequent measurement made directly with a solid ^{15}N target confirmed the validity of the method used to extract the dilution factor.

The beam and target polarizations, P_e and P_p , were routinely monitored during data taking by a Möller polarimeter and a NMR system, respectively. A more precise value of the product $P_e P_p$ was extracted from the simultaneously measured asymmetry for elastic-proton scattering which only depends on the known proton form factors and on the kinematics. Elastic events were selected from the inclusive W spectrum. An independent analysis was performed with elastic events from electron proton coincidences. The results obtained with these different elastic event selections were in excellent agreement. The error due to uncertainties in the parametrization of the form factors was estimated as 1%, and the overall relative accuracy in $P_e P_p$ of 2 – 3% is a significant improvement over the uncertainty associated with separate measurements of P_e and P_p .

FIGURES

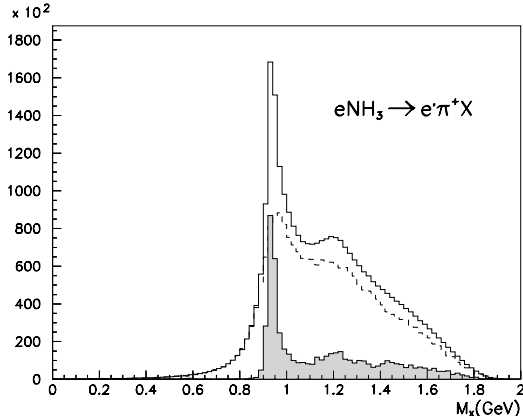


FIG. 1. Missing mass distribution for the reaction $ep \rightarrow e'\pi^+X$. The three overlapping histograms represent the NH_3 (solid line), nuclear background (dashed line), and derived proton (filled histogram) spectra, respectively.

Radiative corrections were calculated using a Monte-Carlo integration of the Mo and Tsai formula [11]. Two different models [12,13] were used to generate the Born cross section and the discrepancy in the final results ($\sim 0.01 - 0.02$) was used as an estimate of the model dependency of the correction.

The total systematic error on the double spin asymmetry due to all sources discussed was estimated to be on the average $\sim 0.05 - 0.06$, which is much smaller than the statistical error.

The double spin asymmetry was evaluated in three Q^2 bins ranging from 0.35 to 1.5 GeV^2 , and in three bins in the angular range $0.25 < \cos\theta^* < 1.0$. For each Q^2 and $\cos\theta^*$ bin, the W dependence was measured from 1.12 GeV up to a maximum of 1.96 GeV . The results were compared to the MAID [12] model and the AO [13] program. MAID and AO are phenomenological models based on parametrization of the existing unpolarized electro-production and photo-production data and can be used to make predictions for polarization observables. For the MAID model the electromagnetic multipoles up to $L = 5$ were used to calculate the helicity amplitudes and the resulting response functions for this process. The cross section terms were integrated over the same bins and acceptance covered by the data in order to provide a direct comparison. A similar procedure was used for the AO calculation,

starting in this case directly from the helicity amplitudes given in this program.

The Q^2 dependence of the asymmetry $(A_1 + \eta A_2)/(1 + \epsilon R)$ integrated over $\cos \theta^*$ is shown in Figure 2 for four W ranges. The dotted curve represents the pure resonance contribution as predicted by the AO model [13], while the solid and dashed lines are respectively the AO and MAID2000 [12] calculations including non-resonant amplitudes. In the low W region, the asymmetry is strongly affected by non-resonant processes, leading to positive values in spite of the negative asymmetry expected for the $P_{33}(1232)$ state. For $W > 1.48$ GeV, the resonance contribution becomes dominant and the asymmetry is positive indicating that the reaction is ruled by the helicity-1/2 amplitude in contrast with the helicity-3/2 dominance observed at the photon point [14]. This feature is consistent with a strong change with Q^2 of the helicity structure of the $D_{13}(1520)$ and $F_{15}(1680)$ states predicted by constituent quark models [1–4] and observed in the unpolarized measurements [15–17]. In the second resonance region ($1.48 < W < 1.6$ GeV) the asymmetry is large already at small Q^2 and slowly approaching saturation, while in the third resonance region ($1.6 < W < 1.72$ GeV) the rise with Q^2 indicates a slower transition from helicity-3/2 to helicity-1/2 dominance due to the underlying $F_{15}(1680)$.

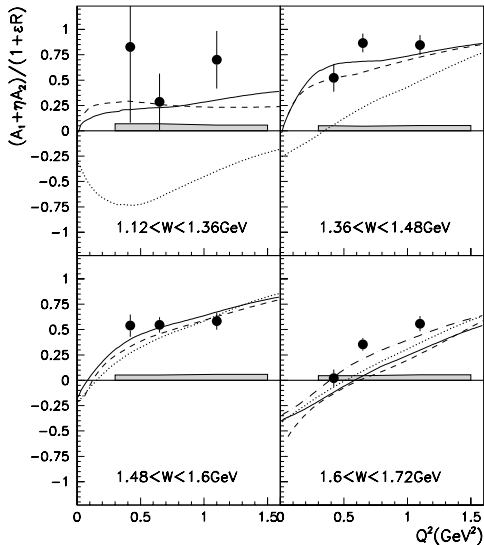


FIG. 2. Q^2 dependence of the double spin asymmetry $(A_1 + \eta A_2)/(1 + \epsilon R)$. The error bars show the statistical error while the shaded area represents the systematic uncertainty. The data are compared with the pure resonance contribution (dotted line) predicted by the AO model, with the MAID (dashed line) and AO (solid line) full calculations, and with the AO prediction obtained with a $\Delta A_1 \sim 0.40$ increase for the $F_{15}(1680)$ (dashed-dotted line).

Additional insight into the helicity structure of the process is provided by the study of the angular distribution. Figure 3 shows the angular dependence of the asymmetry $(A_1 + \eta A_2)/(1 + \epsilon R)$ for $0.5 < Q^2 < 0.9$ GeV² in four different W bins. The rise at forward angles is due to angular momentum conservation that constrains the helicity asymmetry to 1 at $\theta^* = 0$. This is evident in the $P_{33}(1232)$ region where the asymmetry changes sign both because of this constraint and because of the competing contribution of the background which is dominant at forward angles and is predicted to give a positive asymmetry. In Figure 3 the four curves are generated in the same way as in Figure 2. Both models agree fairly well with our results in the low W region. At higher W a systematic discrepancy between the CLAS data and the MAID 2000 prediction appears for the lower $\cos\theta^*$ bin, indicating that the model may underestimate the helicity-1/2 contribution in the second and third resonance regions. A better quantitative agreement is found with the AO calculations. The AO model was modified including a new parametrization of the resonance amplitudes for the $[70, 1^-]$ multiplet based on recent measurements of the photo-coupling for the $S_{11}(1535)$ resonance [18,19] and predicts a larger helicity-1/2 amplitude in the second resonance region than previous parametrizations [20,12] .

A study on the sensitivity to single resonance contributions was performed for the highest W interval. The discrepancy between the data and the model predictions shown both by the Q^2 and the angular dependence for the highest W interval was found to be compatible with a $\Delta A_1 \sim 0.40$ increase for the $F_{15}(1680)$ state included in the AO model. Similar variations applied to other excited states that contribute to this W range did not result in significant improvements in the agreement of the AO calculations with the CLAS data. This result

indicates that the already mentioned transition of the $F_{15}(1680)$ from helicity 3/2 to helicity 1/2 may be more rapid than what is suggested by the unpolarized data, consistent with the prediction of the model of Ref. [3].

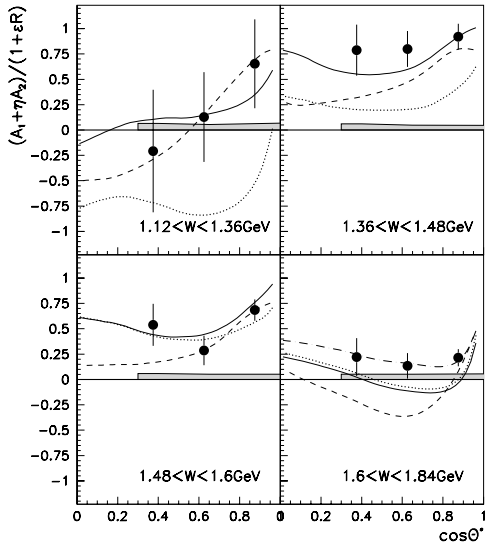


FIG. 3. Angular dependence of the double spin asymmetry $(A_1 + \eta A_2)/(1 + \epsilon R)$ for $0.5 < Q^2 < 0.9 \text{ GeV}^2$. The error bars show the statistical error while the shaded area represents the systematic uncertainty. The curves are the same as in Figure 2.

The double spin asymmetry in the full kinematical range explored by this measurement is given in table I. Both statistical and systematic uncertainties are shown. The latter includes uncertainties of $\sim 0.02 - 0.03$ resulting from the incomplete kinematical coverage. These were estimated using the model of ref. [13].

In conclusion, we have presented the first measurement of the double spin asymmetry for the $\vec{e}\vec{p} \rightarrow e'\pi^+n$ channel. The sign and magnitude of the measured asymmetry indicate the dominance of the helicity-1/2 contribution in the reaction. A comparison with phenomenological models shows the high sensitivity of this observable to resonance contributions. A systematic discrepancy between the MAID model and the CLAS data is present for the second and third resonance region for the lower $\cos\theta^*$ bin. This may indicate an underestimation in the model for the helicity-1/2 contribution in this W range. For $W > 1.6 \text{ GeV}$, the measured asymmetry indicates a faster transition from helicity 3/2 to helicity 1/2

dominance of the $F_{15}(1690)$ resonance compared to the analysis of the unpolarized data.

TABLES

TABLE I. Double Spin Asymmetry results: the three columns correspond respectively to $\cos\theta^*$ in the intervals 0.25-0.5 , 0.5-0.75, and 0.75-1. The asymmetry is expressed in percentage and both statistical and systematic errors are quoted.

$0.35 < Q^2 < 0.5 \text{ GeV}^2$			
$W(\text{GeV})$	$A \pm dA_{st}(A_{sy})$	$A \pm dA_{st}(A_{sy})$	$A \pm dA_{st}(A_{sy})$
1.18	3 ± 38 (5)	-32 ± 29 (5)	56 ± 34 (9)
1.30	24 ± 30 (5)	57 ± 15 (6)	32 ± 11 (6)
1.42	35 ± 13 (8)	30 ± 12 (5)	16 ± 7 (5)
1.54	12 ± 14 (6)	31 ± 11 (5)	31 ± 7 (5)
1.66	-5 ± 15 (5)	-2 ± 9 (5)	1 ± 6 (5)
1.78	-3 ± 27 (6)	-12 ± 18 (6)	5 ± 11 (8)
1.90	-56 ± 29 (7)	6 ± 18 (7)	13 ± 12 (12)
$0.5 < Q^2 < 0.9 \text{ GeV}^2$			
$W(\text{GeV})$	$A \pm dA_{st}(A_{sy})$	$A \pm dA_{st}(A_{sy})$	$A \pm dA_{st}(A_{sy})$
1.18	-41 ± 19 (8)	-15 ± 14 (5)	10 ± 14 (9)
1.30	29 ± 15 (5)	31 ± 9 (6)	45 ± 8 (6)
1.42	40 ± 12 (6)	43 ± 8 (5)	44 ± 6 (5)
1.54	33 ± 12 (6)	22 ± 8 (5)	40 ± 6 (5)
1.66	27 ± 12 (5)	23 ± 8 (5)	23 ± 5 (5)
1.78	5 ± 15 (6)	-7 ± 10 (6)	2 ± 7 (7)
$0.9 < Q^2 < 1.5 \text{ GeV}^2$			
$W(\text{GeV})$	$A \pm dA_{st}(A_{sy})$	$A \pm dA_{st}(A_{sy})$	$A \pm dA_{st}(A_{sy})$
1.18	-15 ± 26 (8)	12 ± 22 (5)	44 ± 21 (6)
1.30	55 ± 17 (6)	55 ± 12 (6)	48 ± 10 (6)
1.42	69 ± 16 (5)	53 ± 11 (5)	49 ± 9 (5)
1.54	28 ± 15 (5)	62 ± 11 (5)	39 ± 8 (5)

Further measurements with beam energy from 1.6 to 5.7 GeV were completed in the Spring of 2001. These data will allow a significant improvement of the statistical precision of this measurement as well as a large expansion of the Q^2 range covered in this study.

We would like to acknowledge the outstanding efforts of the staff of the Accelerator, of the Target Group, and of the Physics Division at TJNAF that made this experiment possible. We are grateful to D. Drechsel and L. Tiator for useful discussions.

This work was supported by the Istituto Nazionale di Fisica Nucleare, the French Commissariat à l'Energie Atomique, the U.S. Department of Energy and National Science Foundation and the Korea Science and Engineering Foundation. The Southeastern Universities Research Association (SURA) operates the Thomas Jefferson National Accelerator Facility for the United States Department of Energy under contract DE-AC05-84ER40150.

REFERENCES

- [1] F. E. Close and Z. Li, *Phys. Rev.*, **D42**, 2194 (1990).
- [2] M. Warns *et al.*, *Phys. Rev.*, **D42**, 2215 (1990).
- [3] S. Capstick, *Phys. Rev.*, **D46**, 2864 (1992).
- [4] M. Aiello *et al.*, *J. Phys.*, **G24**, 753 (1998).
- [5] J. Ahrens *et al.*, *Phys. Rev. Lett.*, **84**, 5950 (2000).
- [6] H. Schmieden *et al.*, *Eur. Phys. J.*, **A1**, 427 (1998).
- [7] M. D. Mestayer *et al.*, *Nucl. Instr. Meth.*, **A449**, 81 (2000).
- [8] G. Adams *et al.*, *Nucl. Instr. Meth.*, **A465**, 414 (2001).
- [9] E. S. Smith *et al.*, *Nucl. Instr. Meth.*, **A432**, 265 (1999).
- [10] M. Amarian *et al.*, *Nucl. Instr. Meth.*, **A460**, 460 (2001).
- [11] L. W. Mo and Y. S. Tsai, *Rev. Mod. Phys.*, **41**, 205(1969).
- [12] D. Drechsel *et al.*, *Nucl. Phys.*, **A645**, 145 (1999).
- [13] V. Burkert and Z. Li, *Phys. Rev.*, **D47**, 46 (1993).
- [14] S. D. Ecklund and R. L. Walker, *Phys. Rev.*, **159**, 1195 (1967).
- [15] H. Breuker *et al.*, *Z. Phys.*, **C13**, 113 (1982); **C17**, 121 (1983).
- [16] E. Evangelides *et al.*, *Nucl. Phys.*, **B71**, 381 (1974).
- [17] W. Brasse *et al.*, *Nucl. Phys.*, **B110**, 410 (1976); **B139**, 37 (1978); V. Gerhardt, Int. Report No. DESY-F21-79/02, 1979 (unpublished); R. Haidan, Int. report No. DEYS-F21-79/03, 1979 (unpublished).
- [18] R. Thompson *et al.*, *Phys. Rev. Lett.*, **86**, 1702 (2001).

- [19] C. S. Armstrong *et al.*, *Phys. Rev.*, **D60**, 052004 (1999).
- [20] V. Burkert, *Czech Journal of Physics*, **46**, 7/8 (1995).